Free-Breathing, Self-Navigated Isotropic 3-D CINE Imaging of the Whole Heart Using Cartesian Sampling

Jens Wetzl[1,2], Felix Lugauer[1], Michaela Schmidt[3], Andreas Maier[1,2], Joachim Hornegger[1,2], and Christoph Forman[3]

[1]Pattern Recognition Lab, Department of Computer Science, Friedrich-Alexander-Universität Erlangen-Nürnberg, Erlangen, Germany, [2]Erlangen Graduate School in Advanced Optical Technologies, Friedrich-Alexander-Universität Erlangen-Nürnberg, Erlangen, Germany, [3]Magnetic Resonance, Product Definition and Innovation, Siemens Healthcare GmbH, Erlangen, Germany

Synopsis

We present a method for free-breathing, isotropic 3-D CINE imaging of the whole heart, demonstrated with experiments in 7 healthy volunteers. Respiratory information for retrospective gating is derived directly from the imaging data. Ventricular function parameters were compared to reference 2-D CINE acquisitions. Excellent image quality and match to ground truth ventricular function parameters could be achieved in an acquisition time similar to multi-slice 2-D CINE with equivalent coverage. Cartesian sampling combined with dual-GPU acceleration enabled a fast reconstruction in under 5 minutes for left-ventricular and under 7 minutes for whole heart coverage.

Introduction

The current gold standard for the evaluation of cardiac function is 2-D CINE imaging, commonly acquired in multiple breath-holds, featuring high in-plane resolution, but thick slices. Recently, 3-D CINE acquisitions with isotropic resolution have been proposed, e.g. free-breathing radial 3-D CINE [1], which requires a computationally expensive reconstruction, or single breath-hold Cartesian 3-D CINE [2], which requires patient cooperation and breath-hold capability. To address these limitations, we propose a method for free-breathing, isotropic Cartesian 3-D CINE imaging.

Methods

Free-breathing 3-D CINE imaging in short-axis (SA) orientation was performed in 7 healthy volunteers (1 female, age 30 ± 13) on a $1.5\,\mathrm{T}$ clinical MR scanner (MAGNETOM Aera, Siemens Healthcare, Erlangen, Germany). One acquisition covered just the left ventricle (LV), another covered the whole heart (WH). A 3-D volume-selective, ECG-gated, bSSFP prototype imaging sequence with the following parameters was used: TR = $2.8\,\mathrm{ms}$, TE = $1.2\,\mathrm{ms}$, $\alpha = 38°$, FOV for LV = $395 \times (237 \pm 10) \times (110 \pm 11)\,\mathrm{mm}^3$, FOV for WH = $395 \times (237 \pm 10) \times (153 \pm 16)\,\mathrm{mm}^3$, acquired voxel size $1.9 \times 2.1 \times 2.5\,\mathrm{mm}^3$, interpolated to $(1.9\,\mathrm{mm})^3$, temporal resolution $42\,\mathrm{ms}$, fixed acceleration factor of 2.6 compared to the fully-sampled matrix and a receiver bandwidth of $1000\,\mathrm{Hz/px}$. For signal reception, 18+12 elements of an anterior + posterior local coil matrix were used. For reference, a 12-slice SA 2-D bSSFP acquisition with $\alpha = 54°$ and retrospective ECG gating in multiple breath-holds was performed to cover the LV with similar temporal resolution, identical in-plane resolution and a slice thickness of $8\,\mathrm{mm}$.

Incoherent sub-sampling of the Cartesian phase-encoding plane was achieved with a spiral spokes sampling pattern, where the starting points for readouts within each phase are chosen along a spiral arm, and subsequent spiral arms are rotated by the golden angle (see Figure 1). As the first sample of each spoke is the k-space center, the sequence is suitable for respiratory self-gating [3]. In every such readout, the lung-liver boundary was tracked to obtain a 1-D respiratory signal (see Figure 2). Retrospective respiratory self-gating to end-expiration resulted in an effective undersampling factor of 11 ± 6 for LV and 14 ± 7 for WH 3-D CINE.

After a Fourier transform along the fully sampled readout, prototype image reconstruction for each phase-encoding plane was then performed using the mFISTA algorithm [4] with spatiotemporal wavelet regularization and incorporating two coil sensitivity maps (CSM) per receive channel to deal with wrapping in the phase-encoding direction [5]:

$$\{\hat{\boldsymbol{x}}_1, \hat{\boldsymbol{x}}_2\} = \underset{\{\boldsymbol{x}_1, \boldsymbol{x}_2\}}{\mathrm{argmin}} \sum_c \left\| \boldsymbol{A}\boldsymbol{F}\left(\sum_{i=1}^2 \boldsymbol{S}_{c,i}\boldsymbol{x}_i\right) - \boldsymbol{y}_c \right\|_2^2 + \lambda \sum_{i=1}^2 \|\boldsymbol{W}\boldsymbol{x}_i\|_1,$$

where $\boldsymbol{A}$ is the sampling pattern, $\boldsymbol{F}$ is the Fourier transform, $\boldsymbol{S}_{c,i}$ is the ith CSM belonging to coil c, $\boldsymbol{y}_c$ is the measured data of coil c, $\boldsymbol{W}$ is the wavelet transform and λ is the regularization parameter. This image reconstruction was fully integrated into the scanner software and multi-GPU-accelerated. The optimization was run for 40 iterations with $\lambda = 2 \cdot 10^{-3}$ of the maximum intensity.

For evaluation, we compared the acquisition and reconstruction times, contrast-to-noise ratio (CNR) as well as ventricular function (VF) parameters computed manually from the images of the gold standard 2-D CINE and our proposed 3-D CINE in corresponding slices of both LV data sets.

Results and Discussion

Qualitative results of the LV and WH 3-D CINE are shown in Figure 3. Quantitative results for acquisition time, reconstruction time and CNR are given in Table 1 and for VF parameters in Figure 4.

The high effective undersampling enabled free-breathing isotropic 3-D CINE with an acquisition time similar to the reference 2-D CINE. The lower CNR for 3-D CINE is due to the lower flip angle (because of SAR restrictions) and inflow effects, the latter causing the further drop from LV to WH 3-D CINE. A slight underestimation of the end-diastolic volume in the 3-D CINE, $1.8\,\mathrm{ml}$ on average, is caused by prospective ECG triggering compared to retrospective ECG gating used by the 2-D CINE [6]. The end-systolic volume is overestimated by $1.6\,\mathrm{ml}$ on average, most likely due to temporal regularization during reconstruction.

Conclusions

We have presented free-breathing isotropic Cartesian 3-D CINE of the whole heart, using retrospective respiratory self-gating. Excellent image quality and match to ground truth VF parameters could be achieved (see Figures 3 and 4). Using the described sampling pattern, retrospective data selection can be applied arbitrarily, e.g. it would also allow retrospective ECG gating instead of prospective ECG triggering, as used in the current study. Cartesian sampling combined with dual-GPU acceleration allows image reconstruction in a clinically feasible range of under 5 (7) minutes for LV (WH). An acquisition in sagittal or coronal orientation is also possible and would remove the need to determine the short-axis orientation. Reduced CNR could be addressed using interleaved T_2 preparation pulses [1]. As future work, a reconstruction using data from all respiratory phases with some form of compensation could further shorten the acquisition time.

References

[1] S. Coppo *et al*. "Free-running 4D whole-heart self-navigated golden angle MRI: Initial results". Magn. Reson. Med. 74(5):1306-1316, 2015.

[2] J. Wetzl *et al*. "Isotropic 3-D CINE Imaging with Sub-2mm Resolution in a Single Breath-Hold". Proc. ISMRM \#1011, 2015.

[3] D. Piccini *et al*. "Respiratory self-navigation for whole-heart bright-blood coronary MRI: methods for robust isolation and automatic segmentation of the blood pool". Magn. Reson. Med. 68(2):571-9, 2012.

[4] J. Liu *et al*. "Dynamic cardiac MRI reconstruction with weighted redundant Haar wavelets". Proc. ISMRM \#178, 2012.

[5] M. Uecker *et al*. "ESPIRiT – an eigenvalue approach to autocalibrating parallel MRI: where SENSE meets GRAPPA". Magn. Reson. Med. 71:990–1001, 2014.

[6] G. Vincenti *et al*. "Compressed Sensing Single-Breath-Hold CMR for Fast Quantification of LV Function, Volumes, and Mass". JACC, 7(9):882-92, 2014.
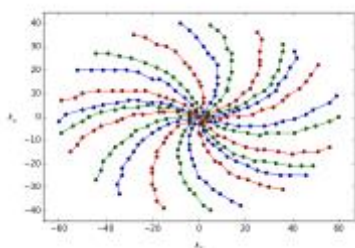
Figures

Figure 1: Undersampling of the Cartesian phase-encoding plane using spiral spokes, in this case for 3 cardiac phases (red, green, blue) with 8 spokes each. Each spoke is the sampled version of a spiral arm, with

starting angles of subsequent spokes being offset by the golden angle. Sampling always begins at the center of k-space.
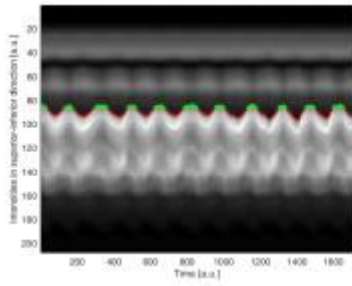

Figure 2: The Fourier transform of k-space center lines acquired over time allows tracking of the lung-liver boundary for retrospective respiratory gating to end-expiration. The red line indicates the tracked boundary, green dots show the accepted sampling locations.
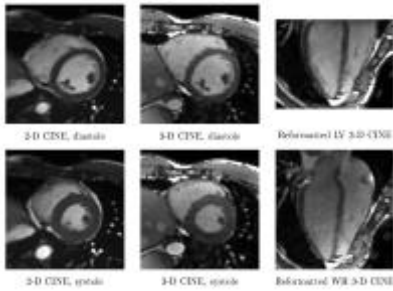

Figure 3: Comparison of 2-D CINE (left column) and 3-D CINE (middle column) short axis slices in diastole (first row) and systole (second row), as well as 3-D CINE images reformatted to horizontal long axis view (right column) for LV (first row) and WH coverage (second row).

	2-D CINE	LV 3-D CINE	WH 3-D CINE
Acquisition time [s]	151 ± 13	172 ± 27	233 ± 32
Reconstruction time [s]	20	255 ± 54	362 ± 80
Contrast-to-noise ratio	14.3 ± 3.7	9.7 ± 2.3	6.6 ± 2.6

Table 1: Comparison of quantitative results for reference 2-D CINE and LV/WH 3-D CINE. The acquisition time for 2-D CINE includes $10\,\mathrm{s}$ breaks between each of the 6 breath-holds. Reconstruction was performed on the CPU for 2-D CINE and on the dual-GPU for 3-D CINE. Contrast-to-noise ratio was measured between the blood pool and myocardium.
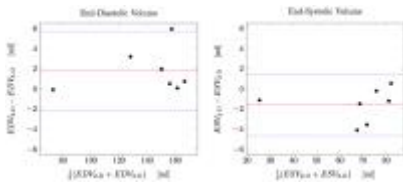

Figure 4: Bland-Altman plots of end-diastolic volume (EDV, left) and end-systolic volume (ESV, right) for the reference 2-D CINE and free-breathing 3-D CINE. Red lines denote the mean difference $E(D/S)V_{\text{2-D}} - E(D/S)V_{\text{3-D}}$, dashed blue lines represent the $95\,\%$ confidence intervals.